# Investigation of the Structure and Properties of Polyisobutylene-Based Telechelic Ionomers of Narrow Molecular Weight Distribution. I.

DON LOVEDAY,[1] GARTH L. WILKES,[1,*] YOUNGKWAN LEE,[2] and ROBSON F. STOREY[2]

[1]Department of Chemical Engineering and Polymer Materials and Interfaces Laboratory, Virginia Polytechnic Institute and State University, Blacksburg, Virginia 24061 and [2]Department of Polymer Science, University of Southern Mississippi, Southern Station, Box 10076, Hattiesburg, Mississippi 39406-0076

**SYNOPSIS**

The solid state morphology of recently developed sulfonated polyisobutylene (PIB) telechelic ionomers with narrow molecular weight distribution (MWD) ($\bar{M}_w/\bar{M}_n \approx 1.15$) was investigated. A small angle X-ray scattering (SAXS) peak often associated with the aggregation of the ionic species in the bulk, as well as a secondary peak, have been observed in the narrow distribution sulfonated PIB telechelic ionomers for the first time. Ionomers of difunctional and tri-arm architecture at several number average molecular weights ($\bar{M}_n$) with one of several counterions were investigated and the preparation method was also considered in terms of observed SAXS behavior. Compression-molded films made from these narrow MWD telechelics were examined in detail using SAXS. Primary and secondary peaks were observed in the slit-smeared SAXS profiles up to an $\bar{M}_n$ of 27 kg/mol. The ratio of the interdomain spacings derived from these peaks (ca. 2 : 1) suggests cylindrical or lamellar ordering in the morphology in both difunctional and tri-arm ionomers. Pinhole SAXS images showed no azimuthal dependence in the scattering pattern and thus, this ordering is on a local scale. It was found that the counterion has an inconsistent effect on the smeared interdomain spacing associated with the SAXS peak. The smeared interdomain spacings were systematic with respect to architecture and $\bar{M}_n$ for solution cast $Cs^+$ ionomers. The difunctional telechelics exhibited higher smeared interdomain spacings than tri-arms of comparable $\bar{M}_n$ and unlike the compression-molded films, the smeared interdomain spacings of the solution cast $Cs^+$ telechelic ionomers increased systematically with increasing $\bar{M}_n$. Even a broad MWD ($\bar{M}_w/\bar{M}_n \approx 1.8$) tri-arm telechelic ionomer $\bar{M}_n$ of 20.6 kg/mol exhibited a diffuse primary peak in SAXS when solution-cast. However, it exhibited no peak when compression-molded. 

## INTRODUCTION

Ionomers are macromolecules which are predominantly of a nonpolar nature but contain ionic functionality as an integral part of the chain at typically less than ca. 15 mol %. Traditional ionomers have randomly placed ionic moieties and models have been developed to describe their structure–property relationships.[1–9] However, a general consensus as to the correct model of ionomer structure and properties is lacking, though the model put forth by Eisenberg, Hird, and Moore[9] seems to be the most acceptable for random ionomers. Interest has developed in controlling the location of the ionic functionality on the polymer chain, such as in segmented,[10–13] block,[14–23] and telechelic[24–41] ionomers. In the telechelic ionomers, the ion pair interaction is confined to the end(s) of the macromolecule. Typical forms of the telechelic ionomers found in the literature are shown in Figure 1. Using telechelic ionomers

* To whom correspondence should be addressed.

Journal of Applied Polymer Science, Vol. 63, 497–506 (1997)
 CCC 0021-8995/97/040497-10

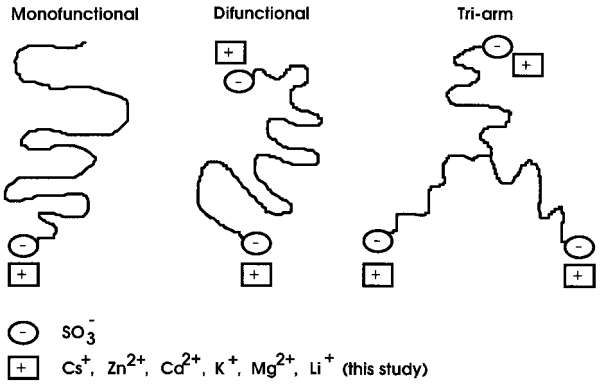


**Figure 1** Schematic of the architecture of common types of sulfonated telechelic ionomer.

which are amorphous and elastomeric in nature, one can potentially elucidate the effect of the ionic aggregates associated with the properties of ionomers without the ambiguity inherent in the use of random ionomer systems. Specifically, in tri-arm sulfonated polyisobutylene (PIB) telechelic ionomers the aggregation of the ionic species in the solid state can result in the formation of a thermally reversible rubbery network structure. This structure has been used to examine in detail the network properties of ionomer systems.[30–36]

Some telechelic ionomers have been shown to exhibit ordering on the level of simple aggregates of ionic groups[25] or higher ordering,[26–28] though the latter occur only in the case of mono or difunctional telechelics. Venkateshwaran et al. found that sulfonated polyisoprene (PIP) difunctional telechelics with either carboxylate or sulfonate ends and neutralized with various counterions exhibited a single, strong SAXS scattering peak[25] without higher orders of scattering. (It should be noted that although the polydispersity of the MWD in these difunctional PIP materials was not stated, they were prepared by anionic techniques and should therefore be relatively monodisperse, with an $\bar{M}_n$ of 15 kg/mol.) On the other hand, Shen et al.[26] found extensive ordering in *monofunctional* PIP sulfozwitterions with lower $\bar{M}_n$ materials ($\leq$4.6 kg/mol) exhibiting arrays of ionic cylinders on a triangular lattice. In materials of more substantial $\bar{M}_n$ ($\geq$14 kg/mol), they observed SAXS profiles which indicated a body centered cubic lattice with lattice spacings that increased with increasing $\bar{M}_n$. Difunctional telechelic polymers based on PIP and terminated with $Ca^{2+}$ and $Ba^{2+}$ carboxylic acid salts have also been found to exhibit a single SAXS peak.[27] Difunctional polybutadiene (PBD) telechelics of broad MWD ($\bar{M}_w/\bar{M}_n \approx 1.8$) terminated with carboxylic acid salts of various counterions also exhibit higher orders of scattering.[27,28] In studies of difunctional PBD-based halato telechelics at a relatively low $\bar{M}_n$ of ca. 4.6 kg/mol,[28] the relationship between the interdomain spacing and $\bar{M}_n$ led the researchers to assign a lamellar morphology. In studies of higher $\bar{M}_n$ materials of the same type, Williams et al. found another morphology was possible and that an assignment of lamellar domains was unwarranted.[27] In a related study, Moore et al. showed that ordering can occur on a local scale in side-chain ionomers based on PS backbones and 11-carbon alkyl spacers with the ionic group on the tip of the alkyl side chain.[29] This ordering was taken to be the "onset" of the type of telechelic ordering observed in SAXS by Broze et al.[28] or Williams et al.[27] Thus, the side-chains emanating outward from the backbone are pictured by Moore et al. as like the arms of a difunctional telechelic of narrow MWD. On the other hand, consistent peaks have not been reported in the SAXS profiles of sulfonated tri-arm PIB telechelic ionomers to date.[30–36] Note that one very diffuse, weak peak was observed in a single sulfonated $K^+$ tri-arm PIB telechelic of broad MWD ($\bar{M}_w/\bar{M}_n \approx 1.7$) and an $\bar{M}_n$ of 8.3 kg/mol,[36] but no other SAXS peaks have been observed in these ionomers.

Sulfonated PIB-based telechelic ionomers were first synthesized by Kennedy and Storey using the "inifer" method.[37] These original sulfonated PIB telechelic ionomers were of several $\bar{M}_n$s and counterions and had an $\bar{M}_w/\bar{M}_n \approx 1.7$; they exhibited the properties of a thermally reversible network and, with one exception, they did not display a SAXS interference peak.[36] The lack of the SAXS interference peak was puzzling, as this peak is often seen in ionomers and is associated with the presence of ionic aggregates from which the ionomers derive their properties. Bagrodia et al. attributed the lack of a SAXS peak to the low volume fraction of ionic material (less than 2 vol %) and to ionic aggregation only on the level of "multiplets." Recently, Storey and Lee[38] reported the synthesis of telechelic ionomers of narrow MWD ($\bar{M}_w/\bar{M}_n \approx 1.15$) produced by living carbocationic polymerization of isobutylene. This is the first report on the structure of such PIB ionomers where the polydispersity of the molecular weight distribution is controlled and narrow, and the results shed light on the apparent lack of structure in the earlier telechelics, as indicated by SAXS. These materials have a much narrower MWD, relative to the materials studied earlier in the labo-

ratories of Wilkes and Kennedy.[30–37] This research also considers other system variables, such as $\bar{M}_n$, architecture, counterion type, and preparation method. In Part II of this two-part series, the specific structure–property effects of the molecular weight polydispersity in these telechelic systems are also addressed.[39]

## EXPERIMENTAL

The telechelic PIB hydrocarbon precursors with narrow MWD were produced using living carbocationic polymerization, according to published methods.[38,40] Briefly, the initiation system for isobutylene polymerization consisted of either a di or trifunctional cumyl chloride-type initiator, along with the co-initiator $TiCl_4$ and the electron donor pyridine, in a 60/40 (v/v) hexane/methyl chloride solvent mixture at −80°C. The resulting PIBs, possessing two or three tert-alkyl chloride end groups, were reacted directly with acetyl sulfate (4-fold molar excess, relative to PIB end groups) in a 90/10 (v/v) methylene chloride/hexane mixture (higher molecular weight PIBs required slightly higher proportions of hexane for solubility considerations) at room temperature for 3 h. It is important to note that this method represents the direct sulfonation of the tert-alkyl chloride termini, in contrast to the earlier method of Kennedy et al.,[30–37] which involved first dehydrochlorination and then the sulfonation of the resulting olefinic end groups.

Purification of the crude sulfonated polymers was achieved either by ion-exchange column chromatography[38] or conventional flash-precipitation into hot water. Neutralization with each desired counterion ($Cs^+$, $Zn^{2+}$, $Ca^{2+}$, $K^+$, $Mg^{2+}$, or $Li^+$) was carried out to stoichiometric equivalence by dissolving the moist sulfonated polymer into THF (50 mg/mL) and titrating the solution at 50°C (Phloxine B indicator) with an ethanolic solution of the desired metal hydroxide or acetate. The ionomer was isolated by pouring the neutralized solution into a 1 L Teflon resin kettle and evaporating the solvents in an oven at 50°C for 2 days, then drying *in vacuo* for another 3 days at 60°C.

The characteristics of the ionomers utilized in this study are shown in Table I. The films used in this study were prepared from the telechelic ionomers by two methods. The first method consisted of compression-molding solvent-free polymer crumb between two Teflon sheets separated by steel shims for ca. 20 min at 130°C. The second was solution casting the ionomers from 95/5 (v/v) THF/methanol into Teflon trays, followed by air drying. The resultant films were then dried in the vacuum oven at 110°C for 4 h. A "blend" triarm ionomer was made from several narrow MWD ionomers so that the overall MWD was very close to that of the "true" broad MWD ($\bar{M}_w/\bar{M}_n \approx 1.8$) ionomers which were made by the older dehydrochlorination-sulfonation method, as described before. This "blend" ionomer had a $K^+$ counterion and an $\bar{M}_n$ of 21.4 kg/mol and was made by mixing together four narrow MWD ionomers of different $\bar{M}_n$ in solution, as follows: 30 wt % 11.8; 18 wt % 20.4; 11 wt % 27; 41 wt % 49.5 kg/mol. The "blend" solution was mixed, cast, dried, and compression-molded, as before. A portion of each cesium ionomer film was redissolved in the 95/5 solvent mixture and heated to reflux (reflux was used to try to totally dissolve the telechelics of $\bar{M}_n \leq 20$ kg/mol). It was noted, however, that even 5 or 6 h of reflux in a stirred flask under $N_2$ purge at 80°C was insufficient to fully dissolve the ionomers of $\bar{M}_n$ 10.3 and 11.8 kg/mol. Again, these refluxed films were cast into Teflon trays and covered so that they would dry as slowly as possible (taking approximately 4 days to dry to the touch). As before, these films were dried in a vacuum oven for 4 h at 100°C. All films were stored in a desiccator until the time of testing to avoid moisture problems. The nomenclature for the samples used in this study is given by the following example: 3-20.4-K refers to a tri-arm telechelic with an $\bar{M}_n$ of 20.4 kg/mol and $K^+$ counterion. Table I summarizes the characteristics of the ionomers used in this study.

Small-angle X-ray scattering (SAXS) experiments were done using a Kratky camera, equipped with a Braun position-sensitive detector and supplied with Ni-filtered Cu $K_\alpha$ radiation ($\lambda$ = 0.154 nm) by a Philips PW-1729 X-ray generator. The experimental intensities were corrected for sample thickness, absorption, and counting time and were normalized to a Lupolen standard. Other SAXS experiments were done using a Warhus camera with 0.015″ pinholes in double collimation and Cu $K_\alpha$ X-rays supplied by a Philips PW-1720 generator.

## RESULTS AND DISCUSSION

### Structural Features of the Compression-Molded Telechelic Ionomers

As an example of the SAXS behavior of the difunctional telechelic ionomers, the log–log SAXS pro-

**Table I Molecular Characteristics of the Telechelic Ionomers Studied**

| $M_n$ (kg/mol) | Architecture | Counterions | $M_W/M_n$ |
|---|---|---|---|
| 10.3 | Disfunctional | $Cs^+$, $Zn^{2+}$, $Ca^{2+}$, $K^+$, $Mg^{2+}$, $Li^+$ | 1.15 |
| 19.3 | Disfunctional | Same | 1.15 |
| 11.6 | Tri-arm | $Cs^+$, $Zn^{2+}$, $K^+$, $Mg^{2+}$ | 1.8 |
| 11.8 | Tri-arm | $Cs^+$, $Zn^{2+}$, $Ca^{2+}$, $K^+$, $Mg^{2+}$, $Li^+$ | 1.15 |
| 20.4 | Tri-arm | Same | 1.15 |
| 20.6 | Tri-arm | $Cs^+$, $Zn^{2+}$, $K^+$, $Mg^{2+}$ | 1.8 |
| 21.4[a] | Tri-arm | $K^+$ | 1.8 (blend) |
| 27 | Tri-arm | $Cs^+$, $Zn^{2+}$, $Ca^{2+}$, $K^+$, $Mg^{2+}$, $Li^+$ | 1.15 |
| 49.5 | Tri-arm | Same | 1.15 |

[a] This ionomer is made by blending together four other ionomers, as noted in the text.

files of the specimens with an $\bar{M}_n$ of 10.3 kg/mol are shown in Figure 2; the log intensity–log "s" plot enhances the visibility of the peaks in the SAXS profile. (To minimize the number of figures, only essential SAXS profiles will be shown.) The intensity is plotted as a function of the angular variable, $s$, where $s = (2/\lambda)\sin(\theta)$ and $\theta$ is one-half the radial scattering angle. Desmearing was not performed on the intensities. The interdomain spacings from the peak intensities in the smeared SAXS profiles for the difunctional telechelic ionomers, estimated from Bragg's relation, are listed in Tables II and III. While the secondary SAXS peaks are shoulder-like, they exhibit local maxima which are quite evident. Estimated interdomain spacings were determined by reading these local maxima in the regions denoted by arrows in the figures. The estimated domain spacings from this observation increase with $\bar{M}_n$, as expected. In the case of the $\bar{M}_n$ 10.3 materials, the interdomain spacings are ca. 9 to 9.5 nm and in the materials with an $\bar{M}_n$ of 19.3 kg/mol, they are ca. 10.5 to 11 nm. It may be noted in the tables that the value of the first peak interdomain spacing, $d1$ is approximately twice that of the second peak interdomain spacing, which, according to Bragg's law, provides evidence of lamellar morphology and is evidence for some degree of longer range ordering. However, the presence of hexagonally packed ionic cylinders cannot be ruled out, since the breadth of the secondary peak prevents exact specification of the morphology. It should be noted that hexagonally close-packed cylinders would potentially exhibit two secondary peaks, one at $d1/\sqrt{3}$ and another at $d1/\sqrt{4}$. Thus, there can be no unambiguous peak assignment, given the breadth of the secondary peak, which covers both $d1/\sqrt{3}$ and $d1/\sqrt{4}$.

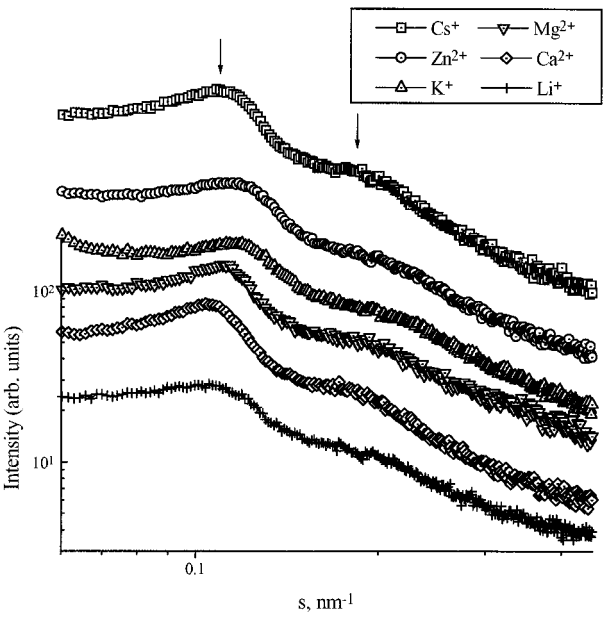


**Figure 2** $\log(I)-\log(s)$ Smeared Kratky SAXS profiles of difunctional sulfonated PIB telechelics with an $\bar{M}_n$ of 10.3 kg/mol. Arrows denote peak regions from which interdomain spacings are derived. Constant offset factor.

To further illuminate the question of macroscopic morphological ordering, a specimen of difunctional $Cs^+$ ionomer with an $\bar{M}_n$ of 10.3 kg/mol was examined both parallel and perpendicular to the film plane normal in a Warhus pinhole camera using Cu $K_\alpha$ radiation. The image collected with the X-rays passing through the specimen along the same axis as in the Kratky camera (that is, along the film normal) is shown in Figure 3, where it is very clear that there are strong primary and secondary maxima. The Bragg spacings estimated from this image are ca. 7.2 and 4.3 nm, respec-

**Table II SAXS Smeared Interdomain Spacings for Compression-Molded Narrow MWD Difunctional PIB Telechelics with an $\bar{M}_n$ of 10.3 kg/mol**

| Counterion | d1 (nm) | $I_1$[a] | d2 (nm) | $I_2$[a] | d1/d2 |
|---|---|---|---|---|---|
| $Cs^+$ | 9.3 | 123 | 5.0 | 38 | 1.9 |
| $Zn^{2+}$ | 9.0 | 56 | 5.0 | 21 | 1.8 |
| $Ca^{2+}$ | 8.9 | 42 | 5.0 | 17 | 1.8 |
| $K^+$ | 9.0 | 52 | 4.9 | 18 | 1.8 |
| $Mg^{2+}$ | 9.6 | 51 | 5.2 | 15 | 1.9 |
| $Li^+$ | 9.9 | 28 | 5.1 | 12 | 1.9 |

[a] $I_1$ and $I_2$ are the primary and secondary peak intensities.

tively. These interdomain spacings are not as close to 2 : 1 (they are 1.7 : 1) as in the Kratky data for either the compression-molded (1.9 : 1; Table II) or the solution cast films (1.8 : 1, see Table VII). A real difference in the ratio of the interdomain spacings may exist between these experiments, simply due to the smearing effect of the Kratky slit collimation. Nonetheless, the lack of azimuthal dependence in this image indicates that there is no macroscopic orientation of the ionic domains and that the ordering is thus on a local scale. (When the Warhus camera pattern is compared with the Kratky SAXS profile, one notes how greatly the Kratky geometry can smear the given scattering profile, thereby considerably reducing or broadening the magnitude of the secondary peak.) The other SAXS image, not shown for brevity, that was taken perpendicular to the film plane normal (that is, parallel to the film surface and through the edge) showed essentially the same pattern as in Figure 3. Thus, the lack of azimuthal dependence in the scattering from at least one of these directions confirms that there is indeed no macroscopic ordering in these telechelic ionomers. It is very unusual to see such structural order with a very low volume fraction of the ionic phase (ca. 1.5 vol %). It should be noted that Feng et al.[10] observed macroscopically ordered rodlike ionic domains in segmented PTMO–dihalide ionenes, where the ionene hard segment was only ca. 8 vol % (PTMO $\bar{M}_n$ 1.8 kg/mol) of the system. Also, Fontaine et al. have observed several orders of scattering in difunctional telechelic $Ba^{2+}$ and $Mg^{2+}$ poly(*t*-butyl acrylate) ionomers of narrow MWD[41]; thus, there are related literature precedents for the high degree of structural order observed in Figure 3 at low volume fraction of the ionic phase.

Returning to Tables II and III, there is no apparent trend relating ion identity to interdomain spacing, though the more massive ions scatter more strongly and have higher peak intensities, as is expected (the ions are listed from higher ($Cs^+$) to lower ($Li^+$) electron density). The intensities of the primary peak are appropriate with respect to $\bar{M}_n$, as the peak intensity should drop with a decrease in the number of scattering centers. Thus, the lower $\bar{M}_n$ difunctional telechelics have higher primary intensities than the higher $\bar{M}_n$ difunctional telechelics for each respective counterion. The 2-10.3-Cs ionomer should have the best ordering and highest X-ray contrast and, in fact, shows strong secondary scattering.

**Table III SAXS Smeared Interdomain Spacings for Compression-Molded Narrow MWD Difunctional PIB Telechelics with an $\bar{M}_n$ of 19.3 kg/mol**

| Counterion | d1 (nm) | $I_1$[a] | d2 (nm) | $I_2$[a] | d1/d2 |
|---|---|---|---|---|---|
| $Cs^+$ | 11 | 117 | 5.6 | 50 | 2.0 |
| $Zn^{2+}$ | 11 | 52 | 6.5 | 25 | 1.7 |
| $Ca^{2+}$ | 10 | 33 | 6.2 | 16 | 1.6 |
| $K^+$ | 10 | 30 | 6.3 | 16 | 1.6 |
| $Mg^{2+}$ | 10 | 19 | 6.2 | 12 | 1.6 |
| $Li^+$ | 11 | 7 | 5.7 | 4 | 1.9 |

[a] $I_1$ and $I_2$ are the primary and secondary peak intensities.

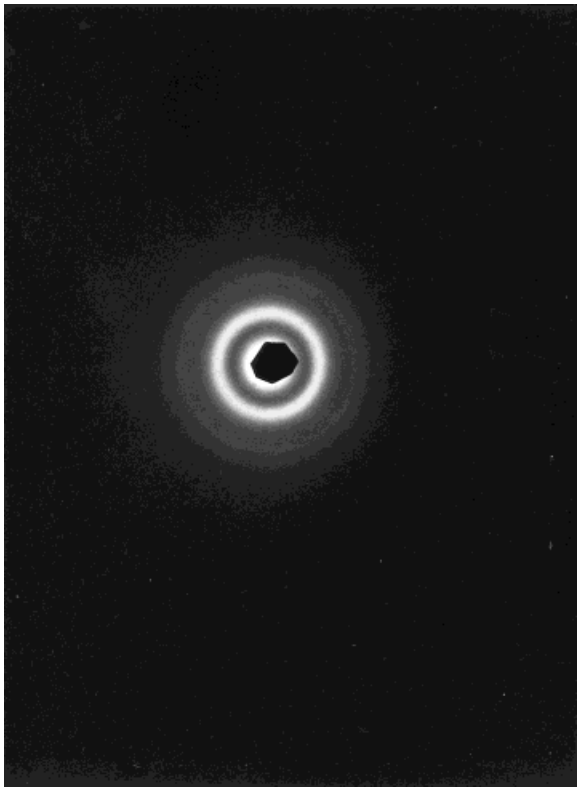

**Figure 3** Warhus SAXS image of the 2-10.3-Cs ionomer along film normal.

The log intensity–log "s" SAXS profiles of some tri-arm materials are shown in Figure 4 and the smeared interdomain spacings are summarized in Tables IV–VI. Just as in the difunctional ionomers, the tri-arm materials also showed no apparent relationship between estimated interdomain spacing and counterion identity. It should also be noted that the ratio of the peak spacings is again ca. 2 : 1, suggesting local secondary structure in the tri-arm telechelic ionomers, such as cylinders or lamellae. Additionally, the peak intensity is not systematic with the mass of the counterion. The interdomain spacing tends to increase with $\bar{M}_n$ in the case of $Li^+$, $K^+$, $Ca^{2+}$, and $Zn^{2+}$, while it apparently decreases for $Cs^+$ and $Mg^{2+}$. Figure 4 (a) and (b) show that the SAXS scattering peaks tend to decrease in visibility with increasing $\bar{M}_n$ until there are no longer any peaks visible. Indeed, none of the 3-49.5 materials displayed a SAXS peak (not shown), and this is thought to be due to the low amount of counterions present in such a system and/or a lack of local secondary structural ordering. Some of the 3-27 materials show an interference peak and some do not. For those that do, the peaks lack sharpness and are diffuse, which are attributed to the relatively low fraction of ionic material (ca. 1 vol %).

The "blend" ionomer 3-21.4-K (described in the Experimental section) was also used to examine the effect of MWD on the morphology of the tri-arm telechelics. While it is not shown here for brevity, the SAXS profile of the "blend" ionomer exhibits a broad peak at an estimated interdo-

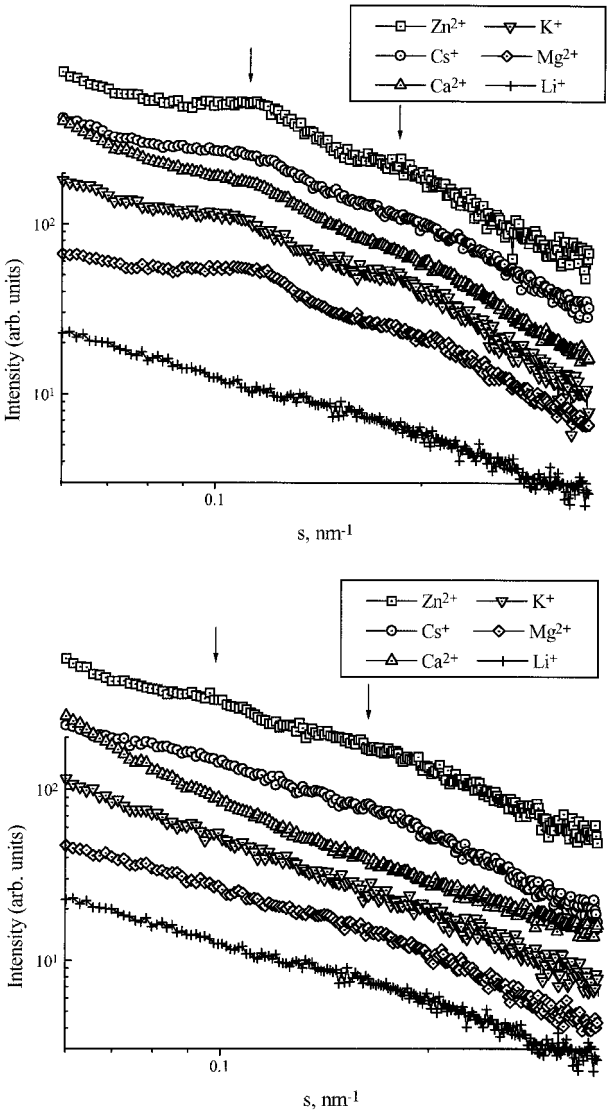


**Figure 4** (a) $\log(I)-\log(s)$ Smeared Kratky SAXS profiles of the tri-arm telechelic ionomers with an $\bar{M}_n$ of 20.4 kg/mol. Arrows denote peak regions from which interdomain spacings are derived. Constant offset factor. (b) $\log(I)-\log(s)$ Smeared Kratky SAXS profiles of the tri-arm telechelic ionomers with an $\bar{M}_n$ of 27 kg/mol. Arrows denote peak regions from which interdomain spacings are derived. A constant offset factor has been used to separate the curves vertically.

**Table IV SAXS Smeared Interdomain Spacings for Compression-Molded Narrow MWD Tri-arm PIB Telechelics with an $\bar{M}_n$ of 11.8 kg/mol**

| Counterion | d1 (nm) | $I_1$[a] | d2 (nm) | $I_2$[a] | d1/d2 |
|---|---|---|---|---|---|
| $Cs^+$ | 9.9 | 420 | 6.7 | 127 | 1.5 |
| $Zn^{2+}$ | 8.2 | 158 | 5.1 | 50 | 1.6 |
| $Ca^{2+}$ | 8.0 | 41 | 5.1 | 19 | 1.6 |
| $K^+$ | 8.9 | 55 | 5.1 | 20 | 1.7 |
| $Mg^{2+}$ | 9.8 | 97 | 5.2 | 19 | 1.9 |
| $Li^+$ | 8.9 | 58 | 5.2 | 18 | 1.7 |

[a] $I_1$ and $I_2$ are the primary and secondary peak intensities.

main spacing of ca. 8.5 nm and no secondary peak. This is strong evidence that the morphological features seen in the current systems are the result of the narrow molecular weight distributions. Even the blended ionomer shows a single, broad interference peak, though its overall MWD is of comparable breadth to the earlier, broad MWD tri-arm PIB ionomers studied by Wilkes et al.[30–36] which showed only one diffuse peak in a single $K^+$ ionomer with an $\bar{M}_n$ of 8.3 kg/mol. Apparently, the local structural ordering due to the individual narrow components is responsible for the observed peak in the SAXS profile.

### Solution Cast Films and Associated Morphology

Often, films cast slowly from solution exhibit morphologies that are different from those found when the same polymer is made into films by compression-molding. In most cases the solution-cast morphology is considered to be nearer the thermodynamically favored equilibrium morphology, since the ionic groups may more easily rearrange themselves in the solution, where mobility is great, than in the less mobile environment of the entangled melt. However, the solvent itself may promote the formation of a distinct morphological form by specific interaction (or lack thereof) with the ionic groups, e.g., by varying the polarity of the solvent, specific effects may be caused in addition to simple dilution. In any case, the solution-cast morphology may be potentially more developed or perfected. To explore this effect, each of the $Cs^+$ ionomers was cast from 95/5 (v/v) THF/MeOH solution and allowed to slowly dry. In Table VII, the spacings associated with the SAXS peaks of both solvent cast and compression molded $Cs^+$ ionomers is contrasted; their scattering profiles are shown in Figure 5. The difunctional telechelics show little apparent difference between the molded and solution-cast materials (allowing 5% standard deviation in the smeared interdomain spacing). Therefore, these difunctional ionomers are likely near their equilibrium morphology even when compression-molded.

In the tri-arm materials, on the other hand, solvent casting resulted in a systematic increase in the smeared interdomain spacing with $\bar{M}_n$. The compression molding process also produced a less systematic change in the interdomain spacing with $\bar{M}_n$, so that reorganization of the ionic domains during molding did not result in the expected trend. Thus, it would seem that the reorganization of the ionic end groups in the melt state

**Table V SAXS Smeared Interdomain Spacings for Compression-Molded Narrow MWD Tri-arm PIB Telechelics with an $\bar{M}_n$ of 20.4 kg/mol**

| Counterion | d1 (nm) | $I_1$[a] | d2 (nm) | $I_2$[a] | d1/d2 |
|---|---|---|---|---|---|
| $Cs^+$ | 9.2 | 65 | 4.7 | 21 | 2.0 |
| $Zn^{2+}$ | 8.9 | 95 | 4.7 | 33 | 1.9 |
| $Ca^{2+}$ | 9.0 | 50 | 4.7 | 17 | 1.9 |
| $K^+$ | 9.4 | 50 | 4.9 | 18 | 1.9 |
| $Mg^{2+}$ | 9.0 | 36 | 4.8 | 14 | 1.9 |
| $Li^+$ | 9.5 | 18 | 5.1 | 8 | 1.9 |

[a] $I_1$ and $I_2$ are the primary and secondary peak intensities.

**Table VI SAXS Smeared Interdomain Spacings for Compression-Molded Narrow MWD Tri-arm PIB Telechelics with an $\bar{M}_n$ of 27 kg/mol**

| Counterion | d1 (nm) | $I_1$[a] | d2 (nm) | $I_2$[a] | d1/d2 |
|---|---|---|---|---|---|
| $Cs^+$ | 11 | 41 | 5.3[b] | 18[b] | 2.1 |
| $Zn^{2+}$ | 12 | 64 | 5.3[b] | 25[b] | 2.2 |
| $Ca^{2+}$ | na[c] | na | na | na | na |
| $K^+$ | na | na | na | na | na |
| $Mg^{2+}$ | na | na | na | na | na |
| $Li^+$ | na | na | na | na | na |

[a] $I_1$ and $I_2$ are the primary and secondary peak intensities.
[b] Estimated value, very diffuse peak.
[c] na = No peak observed.

is more difficult than in the slow casting process, at least for the tri-arm ionomers which suffer from the mobility constraint of the covalent junction point. In Table VII, the ratio of the first and second peak spacings for the solution-cast films is 1.7 : 1 and not ca. 2 : 1, as in the compression-molded materials. It may be recalled that the spacings determined from the pinhole (unsmeared) profile of 2-10.3-Cs (a *difunctional* telechelic), were also 1.7 : 1. However, the difunctional materials should pack more easily into an equilibrium structure than the tri-arms. Thus, the tri-arm materials should not necessarily have the same ratio of interdomain spacings as the difunctional telechelics; they possess the structural and mobility constraint of the central junction. Also, there is potentially an effect due to the distribution of arm lengths in a single tri-arm ionomer, where different combinations of single arm $\bar{M}_n$ can result in the same overall $\bar{M}_n$.

As a comparison to the narrow MWD ionomers, three tri-arm PIB ionomer samples with broad MWD ($\bar{M}_w/\bar{M}_n \approx 1.8$) were newly synthesized using conventional carbocationic polymerization. One of these samples had an $\bar{M}_n$ of 20.6 kg/mol, providing a direct comparison with the narrow MWD sample with an $\bar{M}_n$ of 20.4 kg/mol. The $Cs^+$ broad MWD telechelic ionomer (3-20.6-Cs in Fig. 5) does not show a SAXS peak when compression-molded, though the narrow one does show a peak (3-20.4-Cs in Fig. 5). Furthermore, none of the broad MWD telechelic ionomers showed a peak, regardless of counterion. This absence of a SAXS peak is in agreement with the earlier work of Bagrodia, Wilkes, and Kennedy,[36] which showed that telechelics of broad MWD distribution ($\bar{M}_w/\bar{M}_n \approx 1.7$) exhibited no SAXS peak, except for the single sample, noted earlier. Apparently, under the mobility constraints imposed by the compression molding process, ionomer molecules with a nar-

**Table VII Effect of Film Preparation Method on the Smeared SAXS Interdomain Spacings for the Cesium PIB Telechelic Ionomers**

| Sample | Preparation | d1 (nm) | d2 (nm) | d1/d2 |
|---|---|---|---|---|
| 2-10.3-Cs | Molded | 9.3 | 5.0 | 1.9 |
| 2-19.3-Cs | Molded | 11 | 5.6 | 2.0 |
| 3-11.8-Cs | Molded | 9.9 | 6.7 | 1.5 |
| 3-20.4-Cs, narrow | Molded | 9.2 | 4.7 | 2.0 |
| 3-20.6-Cs, broad | Molded | na[a] | na | na |
| 3-27-Cs | Molded | 11[b] | 5.3[b] | 2.1 |
| 2-10.3-Cs | Cast-dry | 8.9 | 4.9 | 1.8 |
| 2-19.3-Cs | Cast-dry | 12 | 6.6 | 1.8 |
| 3-11.8-Cs | Cast-dry | 7.6 | 4.6 | 1.7 |
| 3-20.4-Cs, narrow | Cast-dry | 11 | 6.7 | 1.6 |
| 3-20.6-Cs, broad | Cast-dry | 14[b] | na | na |
| 3-27-Cs | Cast-dry | 12[b] | 7.4[b] | 1.6 |

[a] na = No peak observed or too diffuse to estimate an interdomain spacing.
[b] Very diffuse peak.

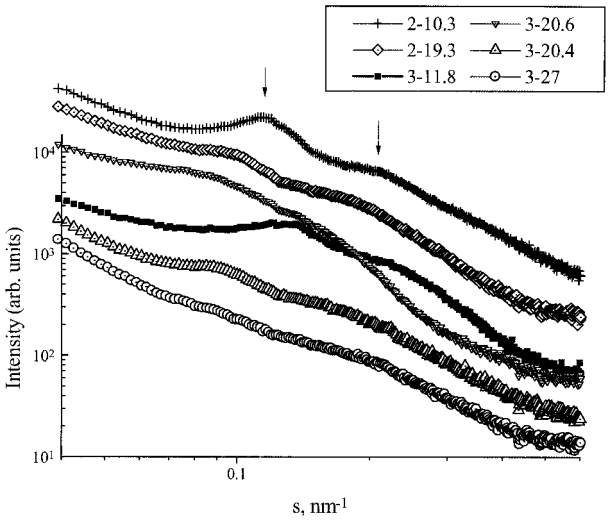


**Figure 5** $\log(I)-\log(s)$ Smeared Kratky SAXS profiles of the tri-arm telechelic ionomers cast from solution. Arrows denote peak regions from which interdomain spacings are derived. Constant offset factor.

row size distribution may more readily pack into a regular, local structure than molecules with a greater size distribution. However, when solution cast in the $Cs^+$ form, the newly synthesized, broad MWD ionomer with $\bar{M}_n$ ca. 20.6 kg/mol did display a peak as shown in Figure 5 and Table VII. This is good evidence that the compression-molding process does not provide adequate chain mobility for the broad MWD triarmionomer molecules to order themselves sufficiently to display a SAXS interference peak. However, the solution casting process clearly does allow the morphological features of the system to develop sufficiently such that the peak is observed.

## CONCLUSIONS

It has been shown for the first time that narrow MWD ($\bar{M}_w/\bar{M}_n \approx 1.15$) sulfonated PIB telechelic ionomers of both difunctional and tri-arm architecture exhibit ordered structure on a local level. This structure is evident as a secondary scattering peak in the SAXS profiles of these narrow MWD ionomers. On the other hand, broad MWD ($\bar{M}_w/\bar{M}_n \approx 1.8$) ionomers of tri-arm architecture do not exhibit even a primary peak when compression-molded. The primary and secondary maxima of the narrow MWD ionomer SAXS profiles exhibit a ratio of estimated interdomain spacings which varies from ca. 2 : 1 to ca. 1.7 : 1. Thus, neither lamellar nor cylindrical morphologies may be unambiguously assigned to these systems. Pinhole SAXS shows that this order is indeed local. It has also been shown that the local arrangement of the ionic domains is dependent on the amount of ionic material in the system. The secondary scattering peak is not observed above an $\bar{M}_n$ of 27 kg/mol. By employing solution casting versus compression molding, one may obtain greater morphological perfection in these systems. This is shown by the fact that the interdomain spacing varies linearly with $\bar{M}_n$ in solution cast materials, though not in compression-molded ionomers. It is also shown by the fact that a broad MWD ionomer exhibits no peak by compression-molding, but does by the solution casting process, where the morphology is presumed to be more developed.

Acknowledgment is made by R. F. Storey to the donors of the Petroleum Research Fund, administered by the American Chemical Society, for partial support of this work.

## REFERENCES

1. A. Eisenberg, *Macromolecules,* **3,** 147 (1970).
2. W. J. MacKnight, T. P. Taggart, and R. S. Stein, *J. Polym. Sci., Polym. Symp.,* **45,** 113 (1974).
3. M. Fujimura, T. Hashimoto, and H. Kawai, *Macromolecules,* **15,** 136 (1982).
4. W. C. Forsman, *Macromolecules,* **15,** 1032 (1982).
5. D. J. Yarusso and S. L. Cooper, *Macromolecules,* **16,** 1871 (1983).
6. D. J. Yarusso and S. L. Cooper, *Polymer,* **26,** 371 (1985).
7. D. Lee, R. A. Register, C. Yang, and S. L. Cooper, *Macromolecules,* **21,** 998 (1988).
8. K. A. Mauritz, *J. Macromol. Sci., Rev. Macromol. Chem. Phys.,* **C28,** 65 (1988).
9. A. Eisenberg, B. Hird, and R. B. Moore, *Macromolecules,* **23,** 4098 (1990).
10. D. Feng, G. L. Wilkes, C. M. Leir, and J. E. Stark, *J. Macromol. Sci., Chem.,* **A26,** 1151 (1989).
11. D. Feng, L. N. Venkateshwaran, G. L. Wilkes, C. M. Leir, and J. E. Stark, *J. Appl. Polym. Sci.,* **37,** 1549 (1989).
12. L. N. Venkateshwaran, G. L. Wilkes, C. M. Leir, and J. E. Stark, *J. Appl. Polym. Sci.,* **43,** 951 (1991).
13. S. A. Visser and S. L. Cooper, *Macromolecules,* **24,** 2576 (1991).
14. R. F. Storey, S. E. George, and M. E. Nelson, *Macromolecules,* **24,** 2920 (1991).

15. R. A. Weiss, A. Sen, C. L. Willis, and L. A. Pottick, *Polymer,* **32,** 1867 (1991).
16. M. Gauthier and A. Eisenberg, *Macromolecules,* **20,** 760 (1987).
17. R. D. Allen, I. Yilgor, and J. E. McGrath, in *Coulombic Interactions in Macromolecular Systems,* A. Eisenberg and F. E. Bailey, Eds., ACS Symposium Series No. 302, American Chemical Society, Washington, DC, 1986.
18. C. D. Deporter, T. E. Long, L. N. Venkateshwaran, G. L. Wilkes, and J. E. McGrath, *Polym. Prepr., Am. Chem. Soc. Div. Polym. Chem.,* **29,** 343 (1988).
19. T. E. Long, R. D. Allen, and J. E. McGrath, in *Chemical Reactions on Polymers,* J. L. Benham and J. Kinstle, Eds., American Chemical Society, Washington, D.C., 1988.
20. J. E. McGrath, J. M. DeSimone, A. M. Hellstern, J. M. Hoover, A. D. Broske, T. E. Long, S. D. Smith, C. Cho, Y. Yu, P. Wood, C. D. Deporter, and J. S. Riffle, in *Multiphase Macromolecular Systems,* B. M. Culbertson, Ed., Plenum Press, New York, 1989.
21. C. D. Deporter, T. E. Long, and J. E. McGrath, *Polym. Intl.,* **33,** 205 (1994).
22. C. D. Deporter, G. M. Ferrence, and J. E. McGrath, *Polym. Prepr., Am. Chem. Soc. Div. Polym. Chem.,* **34,** 574 (1993).
23. L. N. Venkateshwaran, G. A. York, C. D. Deporter, J. E. McGrath, and G. L. Wilkes, *Polymer,* **33,** 2277 (1992).
24. G. Broze, R. Jérôme, and Ph. Teyssié, *Macromolecules,* **15,** 920 (1982).
25. L. N. Venkateshwaran, M. R. Tant, G. L. Wilkes, P. Charlier, and R. Jérôme, *Macromolecules,* **25,** 3996 (1992).
26. Yi. Shen, C. R. Safinya, L. J. Fetters, M. Adam, T. Witten, and N. Hadjichristidis, *Phys. Rev. A,* **43,** 1886 (1991).
27. C. E. Williams, T. P. Russell, R. Jérôme, and J. Horrion, *Macromolecules,* **19,** 2877 (1986).
28. G. Broze, R. Jérôme, Ph. Teyssié, and B. Gallot, *J. Polym. Sci., Polym. Lett. Ed.,* **19,** 415 (1981).
29. R. B. Moore, D. Bittencourt, M. Gauthier, C. E. Williams, and A. Eisenberg, *Macromolecules,* **24,** 1376 (1991).
30. Y. Mohajer, D. Tyagi, G. L. Wilkes, R. F. Storey, and J. P. Kennedy, *Polym. Bull.,* **8,** 47 (1982).
31. S. Bagrodia, Y. Mohajer, G. L. Wilkes, R. F. Storey, and J. P. Kennedy, *Polym. Bull.,* **8,** 281 (1982).
32. S. Bagrodia, Y. Mohajer, G. L. Wilkes, R. F. Storey, and J. P. Kennedy, *Polym. Bull.,* **9,** 174 (1983).
33. Y. Mohajer, S. Bagrodia, G. L. Wilkes, R. F. Storey, and J. P. Kennedy, *J. Appl. Polym. Sci.,* **29,** 1943 (1984).
34. S. Bagrodia, R. Pisipati, G. L. Wilkes, R. F. Storey, and J. P. Kennedy, *J. Appl. Polym. Sci.,* **29,** 3065 (1984).
35. S. Bagrodia, G. L. Wilkes, and J. P. Kennedy, *J. Appl. Polym. Sci.,* **30,** 2179 (1985).
36. S. Bagrodia, G. L. Wilkes, and J. P. Kennedy, *Polymer,* **28,** 2207 (1987).
37. J. P. Kennedy and R. F. Storey, *Org. Coat. Appl. Polym. Sci. Proc.,* **46,** 182 (1982).
38. R. F. Storey and Y. Lee, *J. Polym. Sci. A: Polym. Chem.,* **29,** 317 (1991).
39. D. R. Loveday, G. L. Wilkes, Y. Lee, and R. F. Storey, *J. Appl. Polym. Sci.,* to appear.
40. R. F. Storey and Y. Lee, *J.M.S.-Pure Appl. Chem.,* **A29,** 1017 (1992).
41. F. Fontaine, J. Ledent, R. Sobry, E. François, R. Jérôme, and Ph. Teyssié, *Macromolecules,* **26,** 1480 (1993).

*Received October 31, 1995*
*Accepted June 29, 1996*